Imaging Cortical Structure and Function: New Perspectives for Speech-Language Pathology

Imagerie de la structure et du fonctionnement du cortex : nouvelles perspectives pour l'orthophonie

Kenneth L. Watkin
Department of Biomedical Engineering &
School of Human Communication Disorders
Faculty of Medicine, McGill University

Abstract

The application of imaging technologies to the study of voice production, speech production, speech perception, language, and their associated pathologies is in its infant stages. The potential of imaging methodologies to provide important information on the functioning of the cerebral cortex during speech and language is enormous. Recent studies underscore the need to examine the regional activity of the cortex associated with specific speech and language pathologies. The focus of this report will be to provide a brief introduction to various types of imaging technologies that may be useful in the study of brain-behaviour relationships associated with speech and language performance along with some examples of current research applications using these technologies.

Résumé

L'application des techniques d'imagerie à l'étude de la production de la voix et de la parole, de la perception du langage, du langage et de leurs pathologies en est encore à ses débuts. Les techniques d'imagerie offrent un potentiel énorme pour fournir d'importants renseignements sur le fonctionnement du cortex cérébral durant l'utilisation de la parole et du langage. Des études récentes soulignent la nécessité d'examiner l'activité régionale du cortex qui est liée à certaines pathologies de la parole et du langage. Cet article présente brièvement diverses techniques d'imagerie qui peuvent être utiles pour l'étude des rapports entre le cerveau et le comportement lors de la production verbale, et donne des exemples d'applications actuelles de la recherche à l'aide de ces techniques.

Background

Recent advancements in computer technology and associated graphics hardware capable of providing high resolution colour images have formed the basis for advanced medical imaging systems. Many of these imaging systems now have the capability of providing both two-dimensional (2D) and three-dimensional (3D) projections of various types of physiological and structural information in either grey-scale or colour images. The utilization of such systems in the study of human cognitive functioning, including speech and language production by normal individuals and those with pathologies, is beginning to be undertaken. The focus of this report will be to provide a brief introduction to various types of imaging technologies that may be useful in the study of brain-behaviour relationships associated with speech and language performance along with examples of current research using these technologies.

The current imaging methods employed to study brain-behaviour relationships will be segmented into two distinct categories, those focusing on structure and those focusing on function. Each of these categories will be discussed separately, although from a clinical perspective, both types of information should be used together.

As a three-dimensional structure the human brain and its components have been the subject of considerable research. Descriptions of the regional architecture of the human brain date back to Broca's comparative anatomical studies on the convolutions of the cerebral cortex (Broca, 1878). Such descriptions form the bases for understanding the structural composition of the brain as well as its function. There are two different ways with which the regional structure of the cortex has been described. In the first view, regions of the cortex were subdivided into components based upon structural differences between regions. This resulted in numbered maps of brain regions (Brodmann, 1909; Exner, 1881). A very complex map was proposed by Exner (1881). Brodmann's (1909) classification system was less complex and is still in use. His classification scheme is presented in Figure 1. The second view is based upon an understanding of behavioral patterns and neuronal connectivity determined by neurological testing, CT, and MRI imaging of the cortex. This view (Mesalum, 1985) provides a map with fewer regions based upon neuronal distributions and behavioral data as shown in Figure 2 (see page 185). Both regional classification systems provide a structural foundation for the localization of speech and language behaviour within the cortex.

Figure 1. Brodmann's classification scheme. (A) The lateral perspective of the left hemisphere and (B) the mesio-lateral view of the same hemisphere.

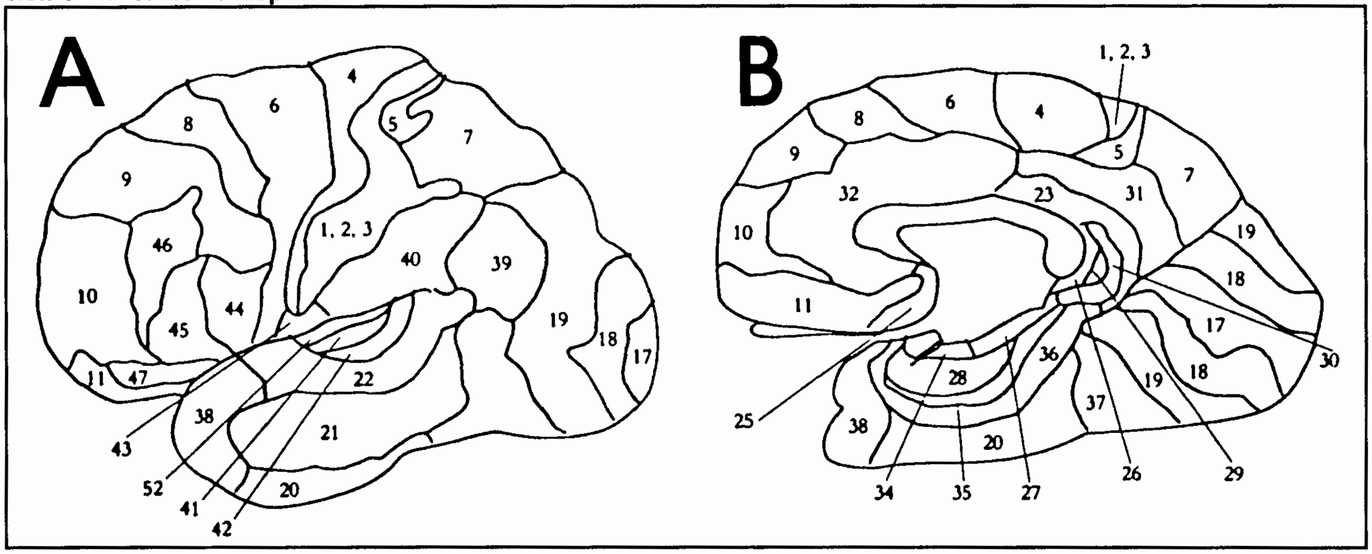

Structural Analysis

The basic technology used to provide structural information on the human body can be subdivided into two broad categories — those that use ionizing radiation and those that do not. A brief description of each type of technology will be presented below along with applications to speech and language pathology.

Ionizing Radiation Sources

Structural descriptions of the human body have been the focus of research since the discovery of x-rays, electromagnetic energy, by William K. Roentgen in 1895. This technology provided a two-dimensional view of internal body structures. Our earliest views of the structure of the human cortex were provided by ionizing radiation sources, x-rays. The basic technology underlying the use of radiated, electromagnetic energy will be presented below. To be useful in the identification of body structures electromagnetic energy must have a wavelength of 0.1 to 0.01 Å and should be attenuated when passing through the body. Although a number of energy sources exist in the x-ray spectrum, only the x-ray tube, in which an electron beam strikes a metal target, has enough intensity to provide an image in a reasonable exposure time. The x-ray energy provided by x-ray tubes is derived from the collisional interactions between electrons and matter. The resulting energy, high-energy photons or x-rays, is accelerated towards the body. The deflected high energy photons are attenuated by the body and the resulting energy is absorbed by a photographic plate. A sample image of the neck and skull is provided in Figure 3. Available in the late 1940s, this type of imaging technology provided a two dimensional sample of the head. In this image we can observe the shape of the skull, the position of the tongue, the hyoid bone, the larynx, and the cortex itself. The problem with this type of image is that it reflects the attenuation of the entire head, that is, it is the sum of all the attenuation provided by the skull and soft tissue. Thus we have a "representation" of the cortex and other structures, but we are unable to visualize small soft tissue regions of the cortex.

In the early 1970's a revolutionary concept was introduced. This imaging concept relied upon computer control of tomographic image acquisition (computed tomography, CT) (Bates, Garden, & Peters, 1983). Introduced first in England, this system provided an isolated image of a slice within a volume, for example, the head, thereby completely eliminating all other view planes. The basic system is presented in Figure 4. An x-ray source is collimated into a narrow beam. This beam is then scanned through the head in a single plane. The transmitted photons are detected by a scanning detector at each position of the scan. This is completed at roughly one degree intervals over a range of 180 degrees. The projected data are sent to a digital computer for two-dimensional display. The scanning planes and their spacing are controlled by computer and set by the operator. Presented in Figure 5 are a sample set of scanning planes used for clinical CT studies. As is readily apparent, the large number of slices provides detailed information on each level of the cortex. Moreover, the morphological differences in the cortex can therefore be examined. The utilization of this technology has begun to provide important information on differences in cortical structure across regions and/or layers, as well as among individuals (Gado, Hadaway, & Frank, 1979; Marrett, Evans, Collins, & Peters, 1989; Pieniadz, Naeser, Koff, & Levine, 1983; Ropper, 1989; Thatcher, Walker, & Guidice, 1987; Walshe, Davis, & Fisher, 1977; Watson, Fleet, Gonzalez-Rothi, & Heilman, 1986; Vallar & Perani, 1986).

Non-ionizing Radiation Sources

Nuclear magnetic resonance (NMR) was discovered by Block, Hansen, and Packard (1946) at Stanford University and by Purcell, Torrey, and Pound (1946) at Harvard University. In 1952 Block and Purcell received the Noble Prize for their independent discovery of NMR. NMR is based on the fact that many atom nuclei have an angular momentum arising from their inherent property of rotation or spin. Such nuclei are electrically charged. Their spin corresponds to the current flowing about their spin axis which generates a small magnetic field. Only nuclei with an odd number of protons or neutrons possess a magnetic moment, exhibit a net spin, and respond to the introduction of an external magnetic field.

Basically the magnetic dipoles of the spinning nuclei will be pointing in a random direction. When placed in a magnetic field the nuclei will orient themselves along the lines of force of the magnetic field. The magnetic behaviour of an entire population of nuclei can be predicted mathematically by defining a single quantity, the bulk magnetization vector, that represents the net effect of all the magnetic moments of the nuclei. When a magnetic field is imposed on the population, the dipoles become oriented in the direction of the applied magnetic field. In the bulk magnetic state the nuclei are spinning much like tiny tops. If the axis of the spinning top is tilted away from the vertical position, the top will rotate about the former (vertical) axis in a motion outlining the wall of a cone; see Figure 6. This motion is called precession (or wobbling). Such tipping can be achieved by applying a much smaller magnetic field at right angles to the static field. In order to tilt the bulk magnetization vector, the frequency of the applied electromagnetic radiation must match the natural precessional frequency of the nuclei, thus the term nuclear magnetic resonance. The electromagnetic radiation used in MNR has a much lower frequency than that used for x-ray radiation sources and therefore does not disrupt the molecules of living substances. In addition, the frequency of the applied electromagnetic radiation field can be "tuned" to different species of nuclei. The tipping of the bulk magnetization vector of an ensemble of nuclei away from its equilibrium position is equal to a transition from a lower energy state to a higher energy state. Once displaced from its original spin axis the nuclei eventually return to the original spin orientation. The properties of the return to their original orientation are called the *relaxation times*. There are different relaxation times, T1 (spin-lattice relaxation) and T2 (spin-spin relaxation). T1 relaxation times reflect changes in the contrast of images, while T2 reflects the changes in the thermal properties of the spin. Variations in the pulse sequences of the electromagnetic radiation source control the T1 and T2 relaxation times. A typical magnetic resonance imaging system (MRI) is shown in Figure 7. Such systems can provide images of a single location, a line, or more commonly a plane or series of planes. Presented in Figure 8 are a sample set of scan planes used in a typical MRI study. A sample MRI image is provided in Figure 9.

Magnetic resonance imaging studies of speech and language have already been initiated. The work of Baer, Gore, Boyce, and Nye (1987)in defining the boundaries of the vocal tract has provided the first MRI views of the speech production apparatus. When applied to cortical functioning, MRI studies have focused on structural patterns or changes in structure (Brownell, Kano, McKinstry, Moskowitz, Rosen, & Brownell, 1991; Graff-Radford, Welsh, & Godersky, 1987; Greitz, Bohm, Holt, & Eriksson, 1991; Jonas, 1981; Kertesz & Ferro, 1984; Kertesz, Lesk, & McCabe, 1977; Wang, Doherty, Hesselink, & Bellugi, 1992). Recently, Plante (1991) and Plante, Swisher, Vance, and Rapcsak (1989) have focussed on the neuroanatomical correlates of specific language impairment. Using MRI, these researchers studied specifically language impaired boys. Plante (1991) results revealed atypical perisylvian asymmetries and disordered language skills. Jernigan, Hesselink, Sowell, and Tallal (1991) have provided additional data on the cerebral structure of language and learning impaired children using MRI techniques. Based on a study of 20 language and learning impaired children who were compared to normal children, they reported significant differences in cerebral asymmetry in the inferior-anterior and superior-posterior cerebral regions. Brain structure volume of the left perisylvian region also was significantly reduced in language and learning impaired children. These results demonstrate that structural studies when applied to specific speech and language populations can provide important information on speech and language development.

It is clear from the examples provided above that MRI has the potential to provide important information on a range of patient ages. Although MRI systems are noisey, the resolution of the image is excellent. For speech studies a special head stabilization mechanism should be used. A holder similar to that reported by Evans, Beil, Marrett, Thompson, and Hakim (1988) would provide necessary stabilization. There are a number of difficulties associated with image measurements. Plante and Turkstra (1991) reported on sources of error in the quantitative analysis of MRI images.

Functional Analyses

Although structural analyses have been used to infer behavioral differences, the techniques discussed above do not provide the type of information we need to understand human behavioral activities. That is, to understand the functioning of the human cortex we need to be able to understand the activity patterns of individual cells or large aggregates of cells. In addition we need to know not only that the cells are active, but also the location of this activity. Current imaging technologies that provide functional analyses of cortical activity fall into two broad categories. One category can be characterized as using invasive techniques, that is, introducing some substance into the body and monitoring the change associated with that substance. The second category can be characterized as non-invasive, that is, no substances enter the body. The presentation below will be segmented into these two categories.

Invasive Techniques

Two of the most important physiological markers of the functioning of the human cortex are the identification of changes in regional cerebral blood flow and regional changes in metabolic activity. Single photon emission computed tomography (SPECT) and positron emission tomography (PET) are the major methods used to image such activity.

SPECT

The use of radioisotopes in tracer quantities for clinical diagnosis of human diseases has grown rapidly during the last decade (Bates, Garden, & Peters, 1983; Alpert, Barker, Gelman, Weise, Senda, & Correia, 1991). Basically, radio-isotope imaging involves the use of radio-nuclide agents that are introduced into the body. These agents, known as *radio-pharmaceuticals*, are designed to demonstrate the physiological function of various organs. Blood flow, blood volume, and a number of metabolic processes determine the distribution of these agents throughout the cortex. The application of this technique began with the use of the radio-isotope ^{133}iodine. This type of imaging utilized a rectilinear scanner and scintillation camera. This device became widely available in the 1960s. The most popular type of imaging equipment used to date to capture radio-isotope is the gamma camera. Unlike standard CT images in which the emission and detection position are known, in radio-isotope imaging only the image detection position can be determined. Thus to create an image, it is necessary to create some form of collimation which defines the direction of the photon. This can be accomplished either mechanically using lead reflectors or electronically. To determine the distribution of the radio-pharmaceutical over time, multiple images are retrieved. This type of imaging, known as *dynamic scintigraphy*, is basic to the use of radio-isotopes. Because radio-isotope images by the very nature of the data gathering process are planar, it is sometimes difficult to determine or localize functional activity within three dimensional organs, such as the human cortex. This has been overcome by taking multiple views during data acquisition, correcting for effects of photon attenuation, and then projecting the distribution of radio-activity. The subject maintains a steady position, a radio-pharmaceutical is injected (into the arm or carotid artery) or inhaled, and then the gamma camera picks up the radio-discharge and creates a display. This image display is usually in colour.

The work of Lasson, Ingvar, and Skinhoj (1978) provides an example of the application of single photon emission computed tomography (SPECT) to the study of cortical functioning. These authors used a multi-crystal single photon tomography to produce single slices of cortical activity. The scanner developed in their laboratories was designed specifically for regional cerebral blood flow studies using ^{133}xenon. Early studies using this radio-nuclide were conducted by injecting the xenon into the carotid artery and recording its uptake using multiple banks of detectors and photomultipliers. Each bank of detectors has photomultipliers arranged in three rows. Thus each scintillator is viewed by three photomultipliers, one in each row. The detectors are position sensitive in the axial direction and use collimators to produce three sections simultaneously. An example of this type of imaging system is presented in Figure 10.

In Lasson, Ingvar, and Skinhoj (1978) ^{133}xenon was injected into the carotid artery. After appropriate uptake time, the gamma cameras were activated and images of cerebral blood flow (CBF) rates were retrieved. These images yield activity within a 1 cm^3 region. Conversion of CBF magnitudes to colour values was used for display purposes. In the colour display in Figure 11, green represents no change in blood flow rate when compare to the resting state and blue indicates a 20% decrease in blood flow rate. The red spectrum is used to code increases of 20% in blood flow rate. In Figure 11, part A was recorded during movements of the contralateral fingers; part B was recorded while counting from 1 to 20 repeatedly; part C was recorded while following a moving visual target; and part D illustrates listening to spoken words. In each case, different cortical centers were characterized by increases in blood flow rate. In part A, blood flow increased along the motor strip as well as in the region of the supplementary motor area. This area is on the medial surface of the hemisphere and above the cingulate gyrus. The gamma camera permits the accumulation of such activity. In part B, counting from 1 to 20, we see three different cortical sites activated. The lower region of the cortex near the isographic regions associated with the tongue, lips, and teeth have increased blood flow along with the supplementary motor area. This is similar but not identical to part A because there is a somatosensory area in the post central gyrus which is also activated. Part C in Figure 11 shows CBF activities associated with following a moving target. The visual association cortex of the occipital cortex, the supplementary motor

Figure 2. Mesalum's classification scheme. *(From Mesalum, 1985, p. 12, reprinted with permission.)*

Distribution of functional zones in relationship to Brodmann's map of the human brain. The boundaries are not intended to be precise. Much of this information is based on experimental evidence obtained from laboratory animals and needs to be confirmed in the human brain. Abbreviations: AA – auditory association cortex; AG – angular gyrus; A1 – primary auditory cortex; CG – cingulate cortex; INS – insula; IPL – inferior parietal lobule; IT – inferior temporal gyrus; MA – motor association cortex; MPO – medial parieto-occipital area; MT – middle temporal gyrus; M1 – primary motor area; OF – orbitofrontal region; PC – pre-frontal cortex; PH – parahippocampal region; PO – parolfactory area; PS – peristriate cortex; RS – retrosplenial area; SA – somatosensory association cortex; SG – supramarginal gyrus; SPL – superior parietal lobule; ST – superior temporal gyrus; S1 – primary somatosensory area; TP – temporopolar cortex; VA – visual association cortex; V1 – primary visual cortex.

Figure 3. A standard lateral projection x-ray image of the head and neck.

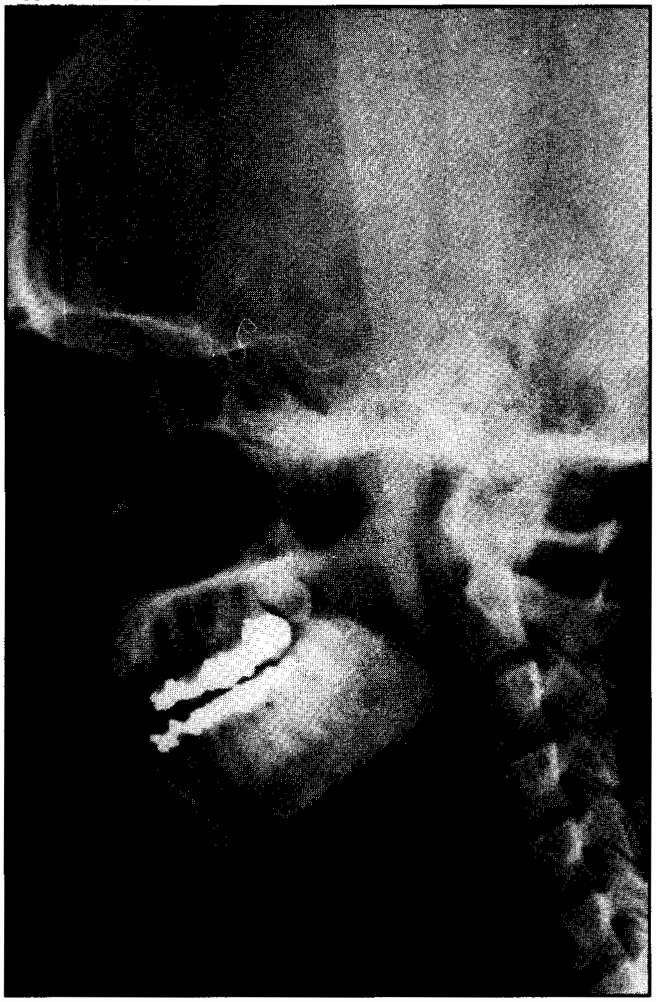

area, and the eye movement regions of the motor strip (for example, the frontal eye field) are all activated. This activation field shows the integration of the somatosensory cortex with the motor cortex for a different activity. Part D is the response of a passive listener. In this task the subject was listening to spoken words and the auditory cortex in the superior temporal gyrus and the adjunct Wernicke's area appear to be activated. One of the main difficulties associated with the use of this technology is that the specific regions activated are large, and therefore we cannot identify detailed regions of activity corresponding to locations on cortical maps such as those proposed by Brodmann. Moreover, we cannot identify with this two-dimensional map the three-dimensional locations of cortical activity. The spatial resolution of the devices as well as the length of time each scan takes are also problems associated with this method. Similar studies using this technology have been reported (Cameron, Modell, Hichwa, Agranoff, & Koeppe, 1990; de la Sayette, Bouvard, Eustache, Chapon, Rivaton, Viader, & Lechevalier, 1989; Bushnell, Gupta, Milcoch, Barnes, & Halsey, 1989; Blauenstein, Wilson, & Wills, 1979; Ingvar & Schwartz, 1974; Jonas, 1981; Knopman, Rubens, Klassen, Meyer, & Niccum, 1980; Larsen, Skinhoj, Soh, Endo, & Lassen, 1977; Larsen, Skinhoj, & Lassen, 1978; Madsen, Holm, Vorstrup, Fribergt, Lasses, & Wildschodtz, 1991; Martin, Friston, Colebatch, & Grackowiak, 1991; Obrist, Thompson, Wang, & Wilkinson, 1975; Raichle, Grubb, Gado, Eichling, & Ter-Pogossian, 1976; Risberg & Ingvar, 1973; Risberg, Ali, Wilson, Wills, & Halsey, 1975; Risberg, Maximilian, & Prohovnik, 1977; Rodrigues, Cogorno, Gris, Marenco, Mesiti, Nobili, & Rosadini, 1989; Roland, & Larsen, 1976; Roland, Larsen, Skinhoj, & Lassen, 1977; Shedlack, Hunter, Wyper, McLuskie, Fink, & Goodwin, 1991; Wood, Taylor, Penny, & Stump, 1980; Wood, McHenry, Roman-Campos, & Poser, 1980).

Recently, Poole, Devous, Freeman, Watson, and Finitzo (1991) have applied this technology to the study of individuals with developmental stuttering (stuttering on-set during childhood). Twenty individuals who stutter were matched with 20 non-stuttering individuals. Regional cerebral blood flow rates during a non-communication task were determined using commercially available SPECT technology. Poole and colleagues report that for stutterers there were reductions in global absolute blood flow. Different relative flow symmetries were identified in three hemispheric regions - the anterior cingulate, superior, and medial temporal gyri. "Milder" changes in the left inferior frontal gyrus were reported. According to Poole and colleagues these findings suggest cortical dysfunction related to reduced and asymmetric left frontal and temporal perfusion.

Terayama, Meyer, Kawamura, and Weathers (1991) measured local cerebral blood flow using enhanced ^{133}xenon on 15 patients with remote cerebral trauma from severe head injury. The patients were divided into two groups, those who improved and those who did not improve 10 years post-

Figure 4. CT imaging system. *(From Webb, 1988, p. 106, reprinted with permission.)*

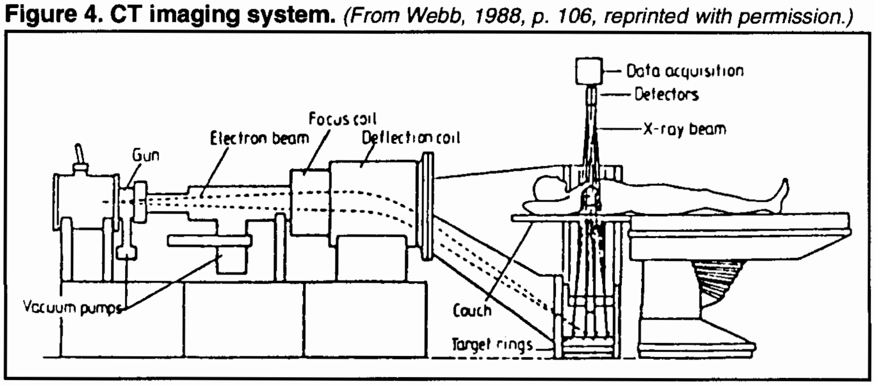

trauma. Subjects were grouped based upon standard cognitive functioning tests. The non-improved group revealed a decrease in frontal and temporal activity and demonstrated reduced blood flow in the region of the putamen, thalamus, and subcortical white matter.

PET

As a tomographic technique, positron emission tomography (PET) developed in parallel to x-ray computed tomography. Quantitative imaging utilizing PET was feasible because of the unique characteristics of positron emitters. Positron emitters are protein-rich isotopes that decay by liberating positrons from their nucleus. The positrons travel short distances during which they lose their kinetic energy when they collide with electrons within tissue. After the positron loses almost all its energy it combines with an electron within the tissue. This sets up an annihilation process that produces two gamma ray photons, each with the energy of 511 KeV. Current imaging equipment provides radiation detectors in a ring about the object monitored to detect the two photons. Thus as the two gamma ray photons are produced as the result of the annihilation process, two detectors opposite each other record the radiation produced by the two gamma ray photons. These occur within a short time period of 5-20 nanoseconds. An example of a ring detection system is presented in Figure 12. Utilization of positrons as a radioactive tracer and electronic collimation were first reported by Wrenn, Good, and Handler (1951). Today's PET scanners instead of having a single ring have multiple levels of staggered rings, which can produce images of the entire organ at one time. The most common radioisotopes used for PET are carbon (^{11}C), oxygen (^{15}O), and Florine (^{18}F). Because of their low positron energy, their contribution to the overall spatial resolution will be small, about 1 mm. Other factors that influence the

Figure 5. CT scans from four patients. *(From Mesalum, 1985, p. 20, reprinted with permission.)*

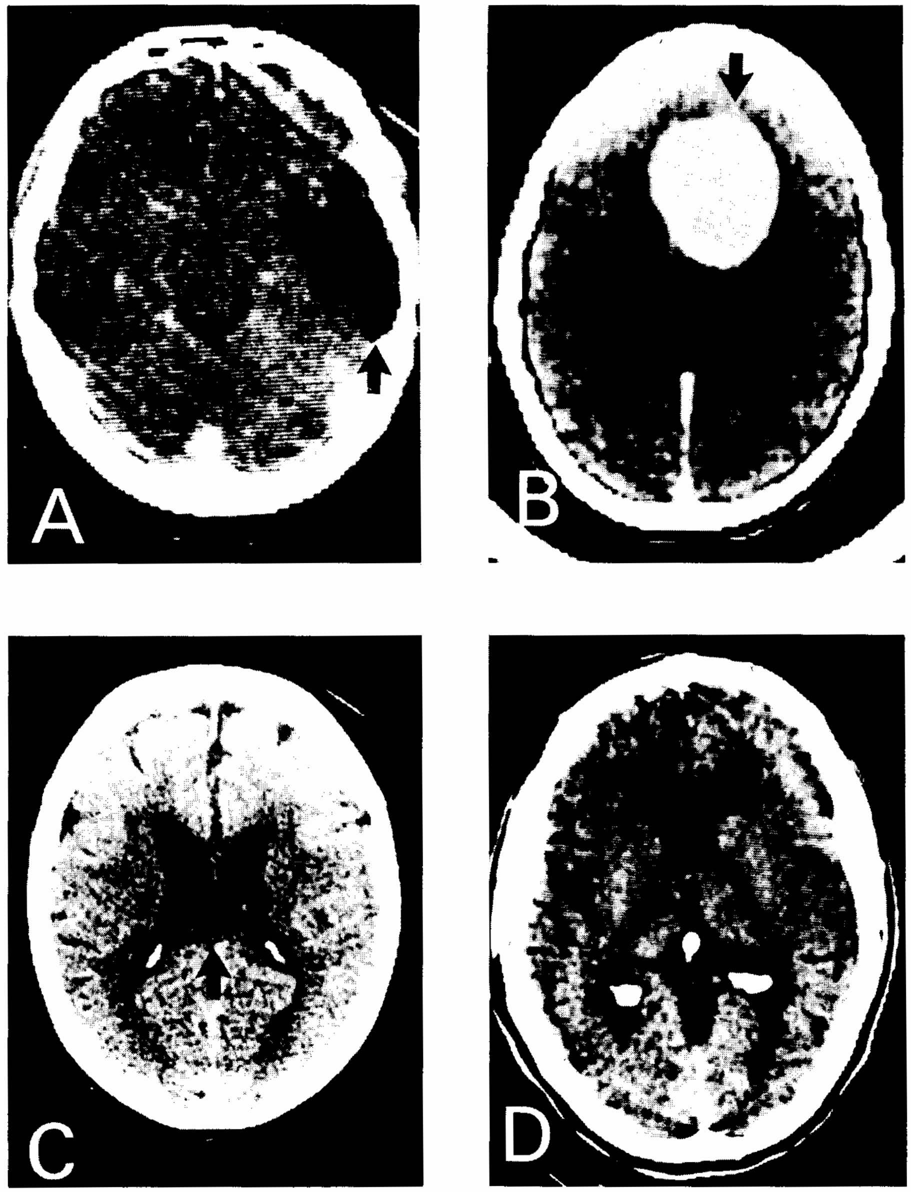

X-ray CT scans from four patients. Left side of the head is on the left side of each scan. (*A*) This 54-year-old right-handed man had a right temporal stroke *(arrow).* The lesion included the superior, middle, and inferior temporal cortex. Salient behavioral deficits included impairments in visual processing and in paralinguistic skills. (*B*) For three years before the discovery of this prefrontal meningioma *(arrow),* this 50-year-old ambidextrous woman carried the diagnosis of an atypical depression with hysterical features. There were essentially no elementary neurologic findings, and most cognitive faculties (e.g., memory and language) appeared preserved. She displayed inappropriate and grandiose behavior and many errors of commission in the go–no-go task. Her behavior and her go–no-go performance both improved markedly after removal of the tumor. (*C*) This 83-year-old right-handed woman had a relatively isolated and progressive amnestic state. The CT scan showed a lipoma of the posterior corpus callosum *(arrow).* (*D*) This 55-year-old right-handed man suffered a lacunar stroke to the left thalamus. The lesion appears to have involved both the anterior nuclear group and the medial part of the medialis dorsalis nucleus of the thalamus *(encircled area).* The patient developed an amnestic condition of moderate severity (mostly for retrieval of verbal material) in conjunction with this lesion.

Figure 6. Cone shape of spin axis where M is the magnetic moment and z is the equilibrium axis.

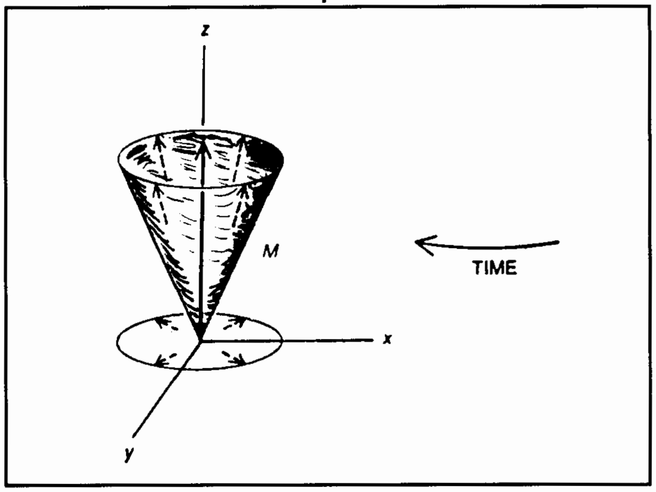

Figure 7. Typical MRI system. *(From Webb, 1988, p. 104, reprinted with permission.)*

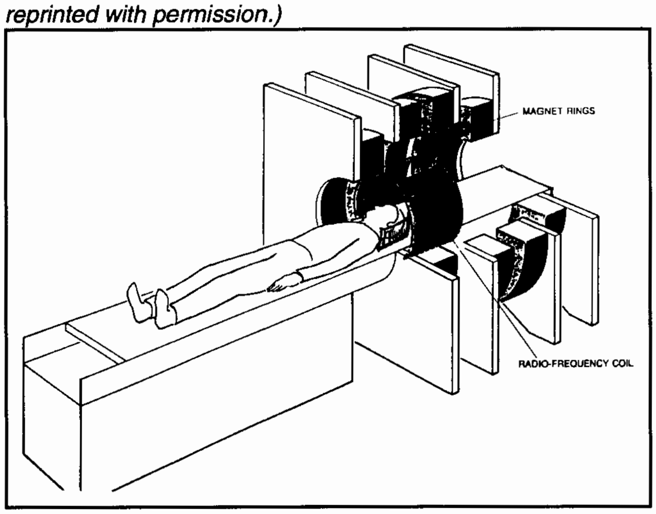

resulting images are positron emission range, angle of positron deviation, photon interactions, scattered radiation, attenuation of photons, and random coincidences. Current monitoring systems provide corrections for each one of these interactions. When compared to current SPECT imaging systems and although more expensive, the PET system allows finer resolution of imaging for both cerebral blood flow and metabolic process imaging. For example, depending upon the intrinsic resolution of the detector and the type of radio-pharmaceutical employed, the resolution of the reconstructed image will range from 2 mm to approximately 8 mm.

The applications of PET are quite diverse (Brownell, Kano, McKinstry, Moskowitz, Rosen, & Brownell, 1991; Evans, Beil, Marrett, Thompson, & Hakim, 1988; Evans, Marrett, Torrescorzo, & Collins, 1991; Fiesche, MacKenzie, Lenzi, Orzi, Iadecola, Lucignani, Di Piero, Pantano, & Pozzilli, 1989; Firth, Friston, Liddle, & Frackowiak, 1991; Foster, Chase,

Figure 8. An example of the cortical axial position of the sampling planes used in a typical imaging system. *(From Evans et al., 1988, reprinted with permission.)*

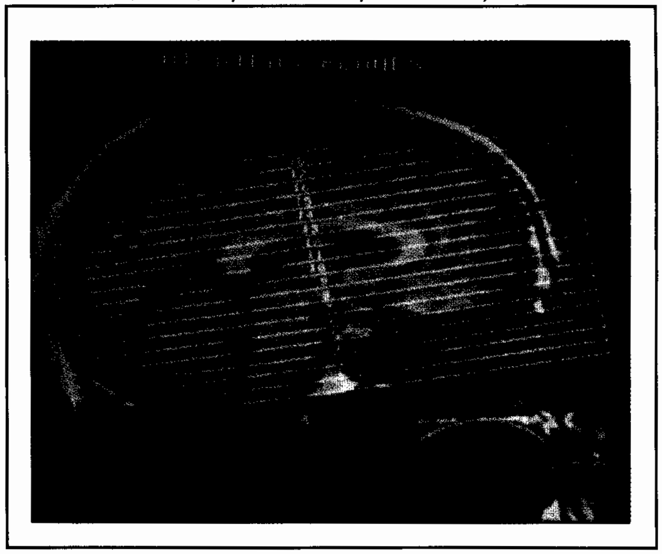

Patrona, Gillespie, & Fedio, 1986; Fiston, Firth, Liddle, & Frackowiak, 1991; Grafton, Mazziotta, Presty, Friston, Frackowiak, & Phelps, 1992; Jamieson & Greenberg, 1989; Mazziotta, Pelizzare, Chen, Bookstein, & Valentino, 1991; Mesalum, 1985; Parks, Lowwenstein, Dodrill, Barker, Yoshii, & Chang, 1988; Petersen, Fox, Posner, Mintun, & Raichle, 1988; Raichle, Grubb, Gado, Eichling, & Ter-Pogossian, 1976). Two organs most frequently studied using PET are the heart and cerebral cortex. Imaging of the cortex can be divided into two categories, static and dynamic.

Static protocols are the most common in a clinical setting. This type of static imaging tends to identify glucose metabolism by using Fluorine18-deoxyglucose (18FDG). 18FDG is usually injected intervenously and about 40 minutes later a single scan of the cortex can be obtained. This represents the cortex's metabolism of glucose. The short positron range of ^{18}F in conjunction with excellent spatial resolution of the gamma camera and sufficient photon activity will yield excellent image quality of the cortex. This type of image can be acquired in a 10-20 minute time period.

Studies of the dynamic changes within the cerebral cortex can also be accomplished using PET systems. PET images can be retrieved in two second intervals or stretched to 30 sec per image. In this kind of dynamic image environment short lived isotopes such as ^{82}Rb and ^{15}O are utilized. This type of study requires higher dosages of radioactivity compared to 18FDG. This is necessary due to the need for higher count rates in the statistical models of the PET system.

Perfusion images created using ^{15}O do not produce ultra-high resolution images. This is due to a large positron range combined with poor photon statistics in the short time interval it takes to retrieve an image. An additional problem accompanying dynamic imaging studies is the amount of data acquired during each study. If images are taken every 5 sec over a 2 min time period, a 21 slice system will produce about 504 images to be analyzed and reconstructed. A subsequent intervention study would require another 504 images, which produces over a 1000 images for reconstruction purposes. This puts significant stress on available computing hardware as well as on projection software.

Some of the major disadvantages to the utilization of SPECT and PET are the potential health hazard of the radio-pharmaceuticals (which precludes many populations), the need to have an on-site cyclotron, subject stability, and the short half life of many of the compounds. However, when SPECT and PET images are linked with region-of-interest maps many significant questions can be addressed (Evans, Beil, Marrett, Thompson, & Hakim, 1988).

Non-invasive Techniques

Electrophysiological techniques also have been used to determine the topographic maps of cortical regions. More recently, with the advent of digital techniques for the acquisition, display, storage and analysis of electroencephalograms (EEG) and/ or stimulus evoked responses (ER), these systems have been called *quantified electro-encephalography* (QEEG). In some cases authors refer to this technology as regional electro-encephalography (REEG).

Most research scientists and clinicians acquiring EEG data adhere to the standards established for traditional EEG applications. Applications tend to use the standard 10-20 International Standard for electrode placement. Most of the QEEG systems use a stimulus averaging technique to enhance their signals. This is used especially in ER systems.

Spatial localization of maximum peak amplitudes has been associated with increased cortical activity (Zappula, 1991). The QEEG cortical mapping system uses a spherical representation of the cortex and colour coding. An example of such a map displaying the first cortical peak of an evoked response of the somatosensory cortex (N20) appears in Figure 13. A sample of the typical evoked responses retrieved is presented in Figure 14. As one can see these time varying waves contain many frequency components. Frequency anal-

Figure 9. Sample MRI image. *(From Webb, 1988, p. 419, reprinted with permission.)*

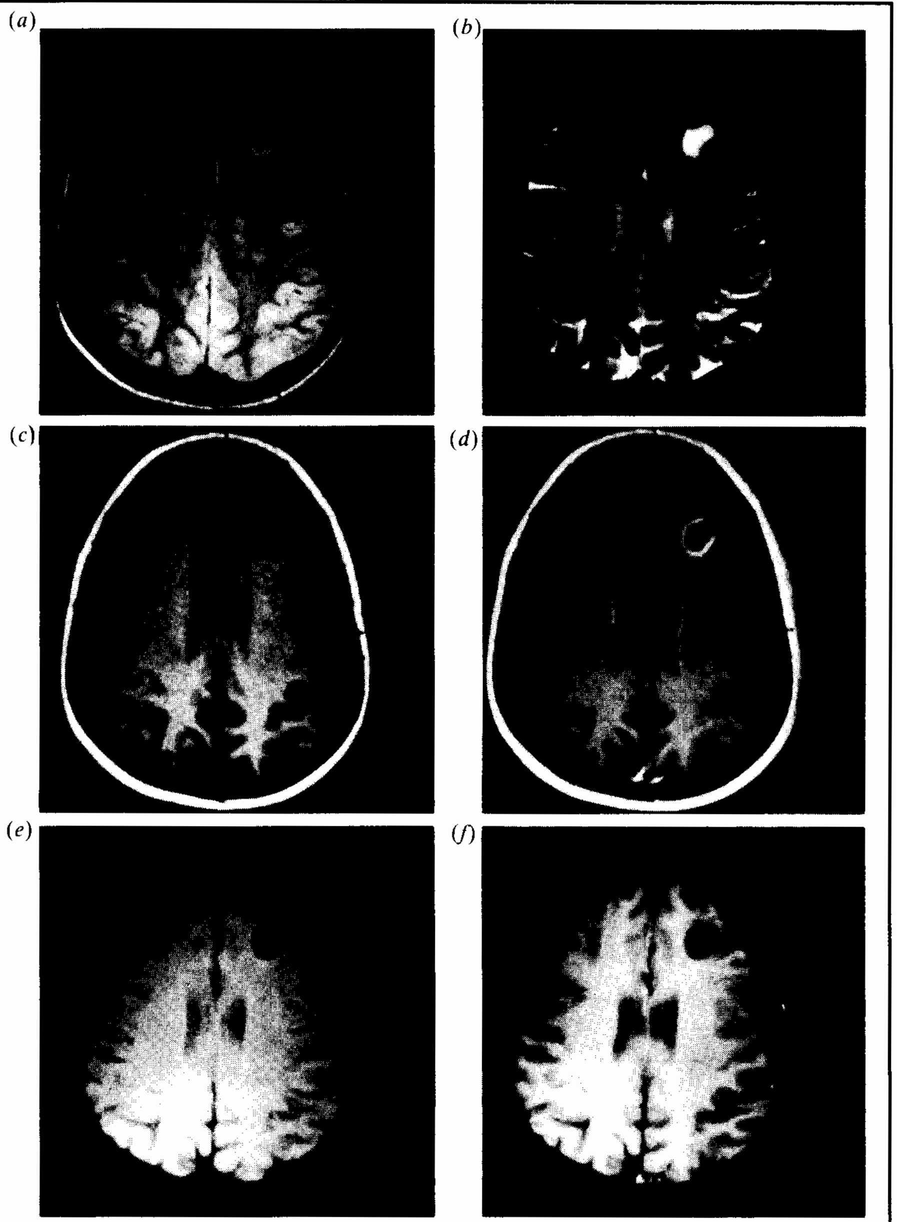

Transaxial images through the brain of a patient with secondary deposits from small cell lung cancer showing the effect of gadolinium DTPA and different sequences on lesion contrast. (*a*) and (*b*) are proton density and T_2-weighted images having T_R = 2.7 s with T_E = 30 ms and 90 ms respectively. (*c*) is a T_1-weighted image with T_R = 0.5 s and T_E = 17 ms. (*d*) is obtained with the same sequence following administration of gadolinium DTPA, which has been taken up in an active ring of tissue at the periphery of the lesion. (*e*) and (*f*) are FLASH 90 and FLASH 50 gradient echo sequences without gadolinium.

Figure 10. Typical SPECT system. *(From Evans et al., 1986, reprinted with permission.)*

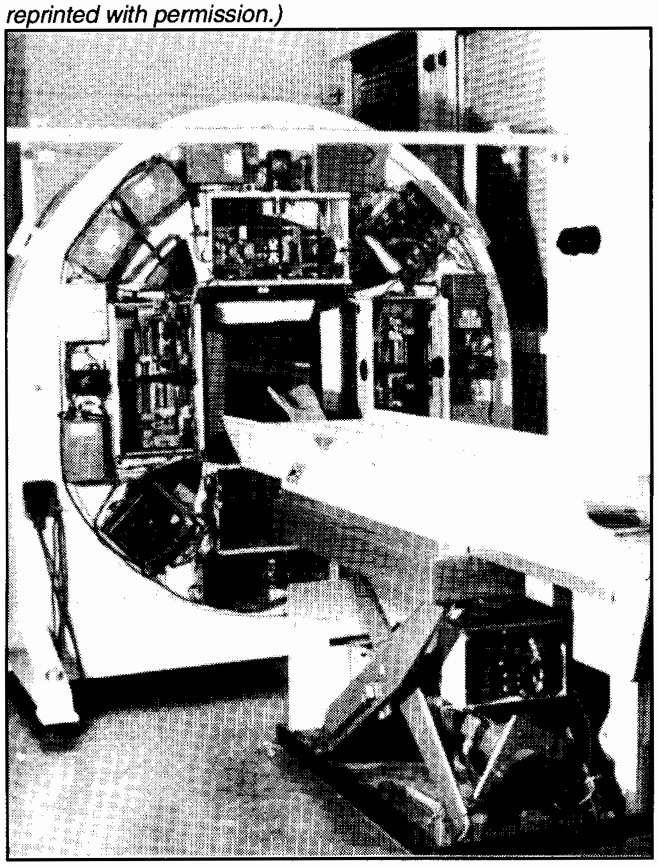

ysis of these components can yield important information. Several different frequency analyses can be performed. The amplitude spectrum, the power spectrum, directional shifts between high and low frequency components associated with changes in cerebral blood flow and metabolism, and power ratios between low (delta and theta) and high (alpha and beta) frequency bands can be determined. In addition to frequency and amplitude measures phased relationships between the component frequencies of a complex wave have also been analyzed. Coherence can also be determined.

QEEG has difficulties worth noting (Kahn, Weiner, Brenner, & Coppola, 1988; Zappulla, 1991). Because recordings are made from the scalp, there is some distortion in the current transmission from the cortex to the scalp electrode site. In addition to this problem, the major drawback to the utilization of QEEG to the study of discrete locations on the cerebral cortex is the location of the electrodes themselves. The large inter-electrode distance and the associated activity at that electrode site, when projected to the cortical map, provide a course mapping of cortical activity. This is readily apparent in Figure 15. More recently researchers have attempted to overcome this difficulty by localizing the electrode source in conjunction with MRI studies of head shape along with the utilization of average head analogues and a 124-channel EEG system (Gevins, Brickett, Costales, Le, & Reutter, 1990; Gevins & Illes, 1991; Thaller, Petsche, Rappelsberger, Pockberger, Lindner, & Imhof, 1991).

Recent application of QEEG to speech and language processing was provided by Gevins and Illes (1991). They utilized a 59 channel EEG recording system. Nine right handed male subjects in good health performed a language task in which they had to judge whether a second visually presented stimulus (S2) for a given stimulus condition formed a match with a first stimulus (S1). Four different conditions were employed: a identity condition, a phonemic condition, a semantic condition, and a grammatical condition. For the identity condition subjects were asked to determine if the two stimuli were identical. In the phonemic condition subjects were asked to determine if the pronounceable but neologistic word stimuli sounded alike. In the semantic condition subjects were asked to decide whether the high frequency open class monosyllabic words were opposite in meaning. In the grammatical condition the subjects were to determine whether an S1 pronoun and S2 verb formed a grammatically correct sentence. Data from this experiment revealed a difference between syntactic and non-syntactic trials in the magnitude of the evoked response potential (ERP). These responses were localized in the anterior frontal and lateral central electrode regions. Additional reports on the application of this technology to speech and language pathology have been provided by Lovrich, Novick, and Vaughn (1988) and Zappulla, LeFever, Jaeger and Bilder (1991).

Another non-invasive method that has the potential to provide additional information about cortical functioning and has been applied recently by a number of researchers is magnetoencephalography (MEG). The detection of biomagnetic fields forms the fundamental technique used by MEG.

The human brain produces electric currents as a result of neuronal activity. These currents create magnetic fields whose intracellular current tangential to the skull contributed to the extracranial magnetic field. This field can be recorded outside the head. These cerebral magnetic fields are very small, approximately 50-500 femtotesla. To record such low amplitude magnetic fields, sensitive transduction devices require a special transduction system. The transducers used are called *SQUID sensors (Superconducting Quantum Interference Device)*. Special shielding with a chamber constructed of aluminum and mu-metal is required to protect against magnetic effects from electrical equipment, power lines, CRTs, and the like (Kelha, Pukki, Peltonen, Penttinen, Ilmoniemi, & Heino, 1982). Fundamental to locating the electrical activity within the brain is the current dipole. A dipole has strength, orientation, and location. Figure 16 depicts the electrical potential patterns and the associated magnetic field produced by a current dipole approximately 20mm below the surface of the skull. In Figure 16 the current dipole is tilted progressively from 0 to 90 degrees to demonstrate the effect on the sensed magnetic field. A schematic representation of this type of a recording system is presented in Figure 17. Early SQUID recording systems used a limited number of SQUID cells (4) immersed in liquid helium. Over 30 SQUID sensor arrays have been constructed (Romani & Pizzella, 1991; Romani, 1990). The greater the number of SQUID recording devices the more precise our ability to record cortical activity. A sample of the cortical activity recorded by each SQUID cell is presented in Figure 18. Like EEG and QEEG, this method of recording cortical activity is rapid and limited only by the time resolution of the recording device. Spatial resolution of the MEG system is approximately 10 mm and is comparable to QEEG methods described above (Cohen, & Cuffin, 1991; Cohen, Cuffine, Yunokuchi, Maniewski, Purcell, Cosgrove, Ives, Kennedy, & Schomer, 1990). The main difference between the two techniques is their ability to record the trangentially or radially oriented components of the dipole. A weak tangential dipole component is difficult to distinguish in QEEG if a strong radial dipole is present (Williamson, Lu, Karron, & Kaufamn, 1991). Strong radially oriented dipoles are difficult to record using MEG. Use of both QEEG and MEG to complement each other has been recommended. An additional limitation of MEG is the cost of the monitoring unit.

Recent applications of magnetoencephalography to cortical functioning has demonstrated its potential role to the study of the initiation of movements as well as cognitive activity. Lange, Cheyne, Kristeva, Beisteiner, Lindinger, and Deeke (1991) studied the current dipoles in the left supplementary motor area (SMA) during voluntary movements of the right thumb by two patients with complete vascular lesions in the right SMA. Left SMA activity was initiated 1200 msec prior to movement onset. Previous MEG studies have failed to localize consistently activity in the SMA prior to movement initiation. Given the results of this investigation it appears that the current dipole sources in the two SMAs may have cancelled each other.

Another application of MEG investigated the cortical responses to speech and non-speech stimuli (Papanicolaou, Rogers, & Baumann, 1991). This technique, patterned after classical evoked potential methodologies, has been attempted recently (Hari, Hamalainen, Kaukoranta, Makela, Joutsiniemi, & Tiihonen, 1989; Kuriki, Murase, & Takeuchi, 1991). Differences in responses to /hei/ compared to noise bursts were reported by Hari and colleagues. The authors attributed the differences to a feature detection process specific to speech sounds. Kuriki, Murase, and Takeuchi, using a variety of speech stimuli (/a/, /ka/, /ba/, /pa/), obtained waveforms similar to those evoked when tonal stimuli were presented. The authors hypothesized that different phonological features initiated different neural units in the auditory cortex. The two studies represent pioneering work in the application of MEG to the study of speech processing.

Conclusion

The application of imaging technologies to the study of voice production, speech production, speech perception, language, and their associated pathologies, is in its infant stages. However, the potential of these imaging methodologies to provide information on the functioning of the cerebral cortex during speech and language is enormous. Recent studies by Jernigan, Hesselink, Sowell, and Tallal (1992) and Plante (1991) underscore the need to examine the regional activity of the cortex associated with specific speech and language pathologies. Many experimental issues need to be addressed. Problems associated with individual variability were recently discussed by Steinmetz and Seitz (1992). Localization of function in the three-dimensional volume of the cortex is especially important. Recently, advanced computer graphics techniques along with low cost computer graphics workstations have the capability of providing three-dimensional images and image reconstructions in reasonable time periods (Mahoney, 1991). The development of 3D cortical mapping systems similar to those described by Pelizzari, Chen, Halpern, Chen, and Cooper (1987), Evans, Beil, Marrett, Thompson, and Hakim (1988), Evans, Marrett, Torrescorzo, and Collins (1991), and Damasio and Frank (1992) provide region of interest and volume of interest atlases based on CT and MRI scans for mapping SPECT and PET data to 3D dimensional data bases (see Figure 19). The integration of these imaging modalities will provide a powerful tool for the study of cortical functioning. The application of the 3D projection software will provide the basis for more precise mapping of cortical activity during various speech and language tasks.

One important aspect in the continued development and utilization of these types of imaging systems is the role of the speech and language scientists and pathologists. To determine the effectiveness of these approaches to our understanding of voice production, speech production, speech perception, language, and their associated pathologies careful research trials need to be conducted. Systematic control of subject populations, imaging technology, and the speech task are essential. Collaborative research efforts can and should form the basis for the application of these technologies in the future.

Address all correspondence to: Kenneth L. Watkin, School of Human Communication Disorders, Faculty of Medicine, McGill University, Montreal, PQ H3G 1A8

Figure 11. ^{133}xenon studies of cerebral blood flow. *(From Lassen, Ingvar, & Skinhoj, 1978, reprinted with permission.)*

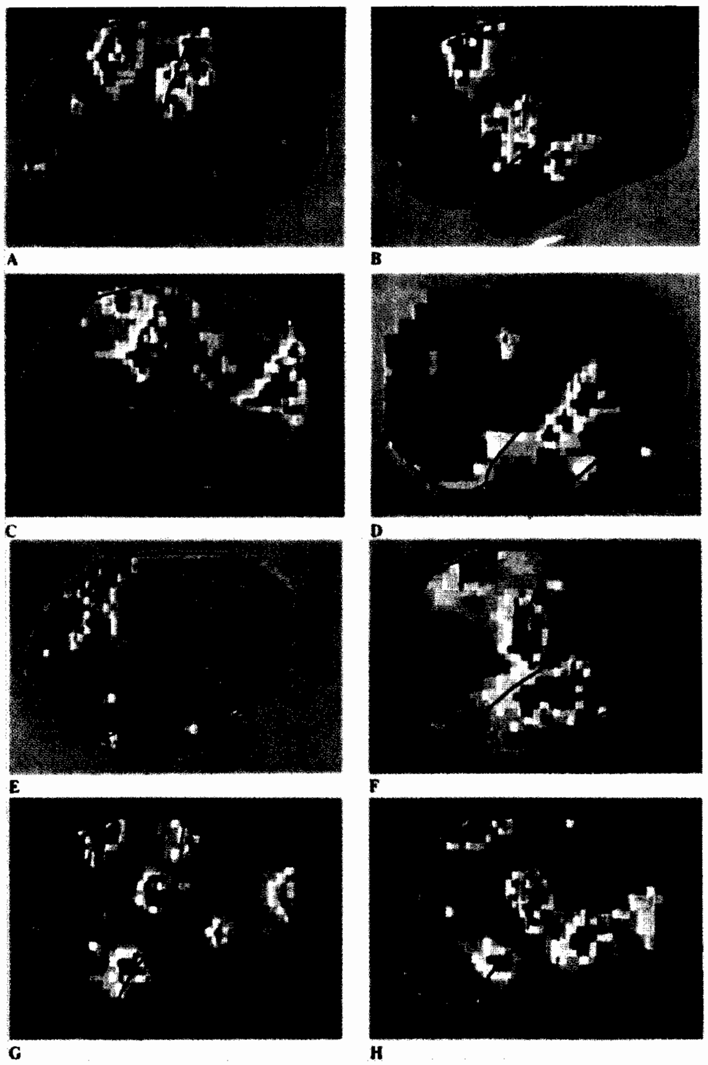

References

Alpert, NM, Barker, WC, Gelman, A, Weise, S, Senda, M, Correia, JA, The precision of positron emission tomography: theory and measurement, *J Cereb Blood Flow Metab*, 1991, *11*:A26-A30.

Bates, RHT, Garden, KL, Peters, TM, Overview of computerized tomography with emphasis on future developments, *Proceeding of the IEEE*, 1983, *71*:533-546.

Baer, T, Gore, JC, Boyce, S, and Nye, PW, Application of MRI to the analysis of speech production, *Magnetic Res Imaging*, 1987, *5*:1-7.

Figure 12. PET ring detector configuration. Diagram of detector configuration in PET systems showing a ring of closely packed detectors. Each detector is in coincidence with several opposite detectors simultaneously as illustrated by the fan beam of coincidence lines of detection for a single detector. *(From Volkow, Mullani, & Bendriem, 1988, reprinted with permission.)*

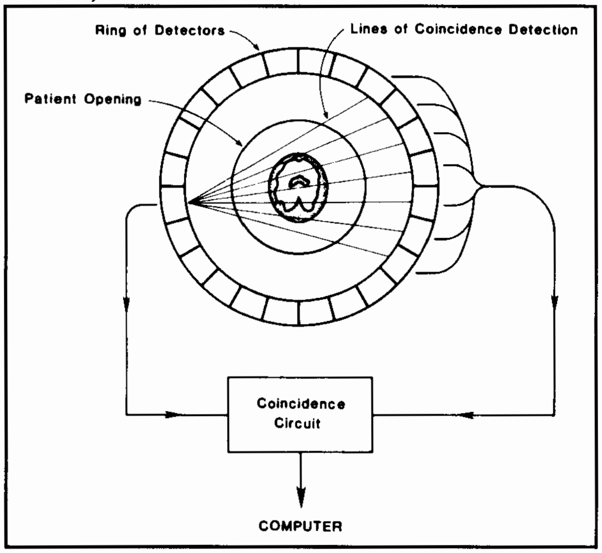

Figure 13. QEEG evoked response map. Tomographic maps constructed for absolute alpha activity for 2. 5, 15, and 30 sec of continuous EEG activity. *(From Zappulla, 1991, reprinted with permission.)*

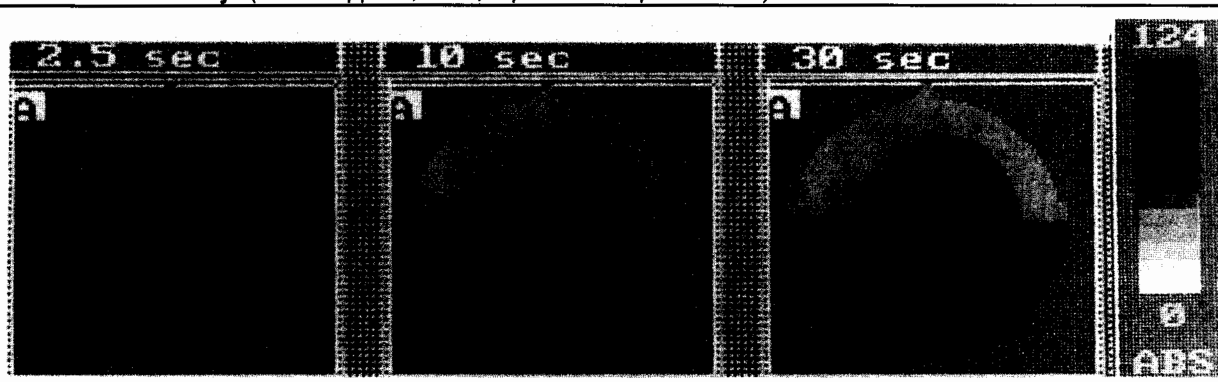

Block, F, Hansen, WW, Packard, ME, Nuclear induction, *Phys Rev*, 1946, *29*:127.

Broca, P, Anatomie comparee des circonvolutions cerebrales: Le grand lobe limbique dans la serie des mammiferes, *Rev Anthropol*, 1878, 1:384-498.

Brodmann, K, *Vergleichende Lokalisationlehre der Grosshirnrinde in ihren Prinzipien dargestellt auf Grund des Zellebaues*, 1909, Leipzig:JA Barth.

Brownell, A-L, Kano, M, McKinstry, RC, Moskowitz, MA, Rosen, BR, Brownell, GL, PET and MR studies of experimental focal stroke, *J Comp Asst Tomog*, 1991, 15:376-380.

Bushneell, DL, Gupta, S, Mlcoch, AG, Bames, WE, Prediction of language and neurologic recovery after cerebral infarction with SPECT imaging using N isopropyl-o- (1123) iodoamphetamine, *Arch Neurol*, 1989, *46*:665-669.

Cameron, OG, Modell, JG, Hichwa, RD, Agranoff, BW, Koeppe, RA, Changes in sensory-cognitive input: effects on cerebral blood flow, *J Cereb Blood Flow Metab*, 1990, *10*:38-42.

Cohen, D, Cuffin, BN, EEG versus MEG locatization accuracy: theory and experiment, *Brain Topogr*, 1991, *4*:95-103.

Cohen, D, Cuffine BN, Yunokuchi, K, Maniewski, R, Purcell, C, Cosgrove, GR, Ives, J, Kennedy, JG, Schomer, DL, MEG versus EEG localization test using implanted sources in the human brain, *Ann Neurol*, 1990, *28*:811-817.

Damasio, H, Frank, R, Three-dimensional in-vivo mapping of brain lesions in humans, *Arch Neurol*, 1992, *49*:137-143.

de la Sayette, V, Bouvard, G, Eustache, F, Chapon, F, Rivaton, F, Viader, F, Lechevalier, B, Infarct of the anterior limb of the right internal capsule causing left motor neglect: case report and cerebral blood flow study, *Cortex*, 1989, *25*:147-154.

Evans, AC, Beil, C, Marrett, S, Thompson, CJ, Hakim, A, Anatomical-functional correlation using an adjustable MRI-based region of interest atlas with positron emission tomography, *J Cereb Blood Flow Metab*, 1988, *8*:513-530.

Evans, AC, Marrett, ES, Torrescorzo, JQS, Collins, L, MRI-PET the correlation in three dimensions using a volume-of-interest (VOI) atlas, *J Cereb Blood Flow Metab*, 1991, *11*:A69-A78.

Evans, NTS, Keys, WI, Smith, D, Coleman, J, Cumpstey, D, Undrill, PE, Ettinger, KV, Ross, K, Norton, MY, Bolton, MP, Smith, FW, and Mallard, JR, The Aberdeen Mark II single-photon-emission tomographic scanner: specification and some clinical applications, *Phy Med Biol*, 1986, *31*:65-78.

Exner, S, *Untersuchungen uber Localisation der Functionen in der Grosshirnrinde des Menschen*, 1881, Vienna:W Braumuller.

Fiesche, C, MacKenzie, E, Lenzi, GL, Orzi, F, Iadecola, C, Lucignani, G, Di Piero, V, Pantano, P, Pozzilli, C, Facts and trends in cerebral blood flow and metabolism: Synopsis of brain '89, *J Cereb Blood Flow Metab*, 1989, 9:573-578.

Firth, CD, Friston, KJ, Liddle, PF, Frackowiak, RSJ, A PET study of word finding, *Neuropsychologica*, 1991, *29*:1137-1148.

Foster, NL, Chase, TN, Patrona, NJ, Gillespie, MM, Fedio, P, Cerebral mapping in apraxia in Alzheimer's disease by positron emission tomography, *Ann Neurol*, 1986, *19*:139-143.

Friston, KT, Frith, CD, Liddle, PF, Frackowiak, RSJ, Comparing functional (PET) images: the assessment of significant change, *J Cereb Blood Flow Metab*, 1991, *11*:690-699.

Gado, M, Hanaway, J, Frank, R, Functional Anatomy of the cerebral cortex by computed tomography, *J Comp Asst Tomog*, 1979, *3*:1-19.

Gevins, AS, Illes, J, Neurocognitive networks of the human brain, in (Ed.) Zappulla, RA, LeFever, FF, Jaeger, J, Bilder, R, *Windows on the Brain*, 1991, *620*:22-44, New York:Annals of the New York Academy of Science.

Gevins, AS, Brickett, P, Costales, B, Le, J, Reutter, B, Beyond topographic mapping : towards functional-anatomical imaging with 124-channel EEGs and 3-D MRIs, *Brain Topogr*, 1990, *3*:53-64.

Graff-Radford, NR, Welsh, K, Godersky, J, Callosal apraxia, *Neurology*, 1987, *37*:100-105.

Grafton, ST, Mazziotta, JC, Presty, S, Friston, KJ, Frackowiak, RSJ, Phelps, ME, Functional anatomy of human procedural learning determined with regional cerebral blood flow and PET, *J Neurosci*, 1992, *12*:2542-2548.

Greitz, T, Bohm, C, Holte, S, Eriksson, L, A computerized brain atlas: construction, anatomical content and some applications, *J Comp Asst Tomog*, 1991, *15*:26-38.

Halsey, JA, Blauenstein, UW, Wison, EM, Wills, EH, Regional cerebral blood flow comparison of right and left hand movement, *Neurology*, 1979, *29*:21-28.

Hari, R, Lounasmaa, OV, Recording and interpretation of cerebral magnetic fields, *Science*, 1989, *244*:432-436.

Hari, R, Hamalainen, M, Kaukoranta, E, Makela, J, Joutsiniemi, SL, Tiihonen, J, Selective listening modifies activity of the human auditory cortex, *Exp Brain Res*, 1989, *74*:463-470.

Ingvar, DH, Schwartz, MS, Blood flow pattems induced in the dominant hemisphere by speech and reading, *Brain*, 1974, *97*:273-288.

Jamieson, DG, Greenberg, JH, Positron emission tomography of the brain, *Computerized Med Imaging Graphics*, 1989, *13*:61-79.

Jemigan, TL, Hesselink, JR, Sowell, E, Tallal, PA, Cerebral Structure on MRI in language- and learning-impaired children, *Arch Neurol*, 1991, *48*:502-519.

Jonas, S, The supplementary motor region and speech emission, *J Communication Dis*, 1981, *14*:349-373.

Kahn, EM, Weiner, RD, Brenner, RP, Coppola, R, Topographic maps of brain electrical activity - pitfalls and precautions, *Biol Psychiatry*, 1988, *23*:628-636.

Kelha, VO, Pukki, JM, Peltonen, RS, Penttinen, AJ, Ilmoniemi, RJ, Heino, JJ, Design, construction and performance of a large volume magnetic shield, *IEEE Trans Magn*, 1982, *18*:260-270.

Kertesz, A, Ferro, JM, Lesion size and location in ideomotor apraxia, *Brain*, 1984, *107*:921-933.

Figure 14. QEEG evoked response map. *(From Zappulla, 1991, reprinted with permission.)*

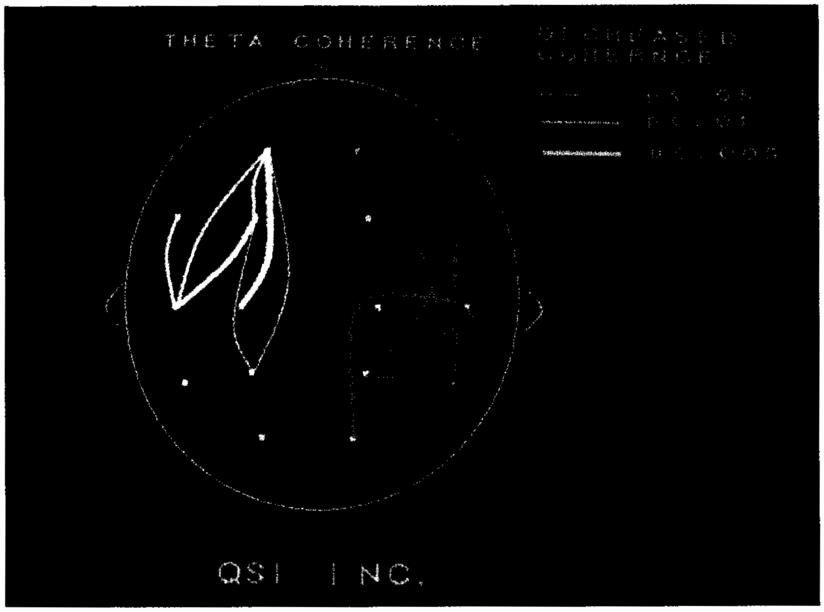

Intrahemispheric coherence plot for a patient with a left frontal tumor. The significance values are derived from comparisons with an age-adjusted normative database.

Kertez, A, Lesk, D, McCabe, P, Isotope localization of infarcts in aphasia, *Arch Neurol*, 1977, *43*:590-601.

Kuriki, S, Murase, M, Takeuchi, Specificity of neurmagnetic responses in the human auditory cortex to consonants of monosyllable speech sounds, In *Advances in Biomagnetism.* Kaufmann, L, Williamson, S, Stroink, G, (Eds.), New York:Plenum Press, 1991.

Knopman, DS, Rubens, AB, Klassen, AC, Meyer, MW, Niccum, N, Regional cerebral blood flow patterns during verbal and nonverbal auditory activation, *Brain and Lang*, 1980, *9*:93-112.

Lang, W, Cheyne, D, Kristeva, R, Beisteiner, R, Lindinger, G, Deecke, L, Three-dimensional localization of SMA activity preceding voluntary movement. A study of electric and magnetic fields in a patient with infarction of the right supplementary motor area, *Exp Brain Res*, 1991, *87*:688-695.

Larsen, B, Skinhoj, E, Lassen, NA, Variations in regional cortical blood flow in the right and left hemispheres during automatic speech, *Brain*, 1978, *101*:193-209.

Larsen, B, Skinhoj, K, Soh, H, Endo, H, Lassen, NA, The pattern of cortical activity provoked by listening and speech revealed by rCBF measurements, *Acta Neurologica Scand*, 1977, *64*:268-269.

Lassen, NA, Ingvar, DH, Skinhoj, E, Brain Function and Blood Flow, *Sci Am*, 1978, *239*:62-71.

Lovrich, D, Novick, B, Vaughn, HG Jr, Topographic analysis of auditory event-related potential associated with acoustic and semantic processing, *Electroencephalogr Clin Neurophysiol*, 1988, *71*:40-54.

Madsen, PL, Holm, S, Vorstrup, S, Fribergt, L, Lasses, NA, Wildschodtz, W, Human regions cerebral blood flow during REM sleep, *J Cereb Blood Flow Metab*, 1991, *11*:502-507.

Mahoney, D P, Picture This[x], *Computer Graphics World*, 1992, *15*:43-52.

Marrett, S, Evans, AC, Collins, L, Peters, TM, A volume of interest (VOI) atlas for the analysis of neuropsychological image data, *SPIE - Medical Image Processing*, 1989, *1092*:467-477.

Martin, AJ, Friston, KJ, Colebatch, JG, Grackowiak, RSJ, Decreases in regional cerebral blood flow with normal aging, *J Cereb Blood Flow Metab*, 1991, *11*:684-689.

Mazziotta, JC, Pelizzare, CC, Chen, GT, Bookstein, FL, Valentino, D, Region of interest issues: the relationship between structure and function in the brain, *J Cereb Blood Flow Metab*, 1991, *11*:A51-A56.

Mesulam, M-M, *Principles of Behavioral Neurology*, 1985, Philadelphia:F A Davis Comp.

McLaughlin, T, Steinberg, B, Christensen, B, Law, I, Parving, A, Friberg, L, Potential language and attentional networks revealed through Factor Analysis of rCBF data measured with SPECT, *J Cereb Blood Flow Metab*, 1992, *12*:535-545.

Obrist, WD, Thompson, HK, Wang, HS, Wilkinson, WE, Regional cerebral blood flow estimated by ^{133}xenon inhalation, *Stroke*, 1975, *6*:245-256.

Papanicolaou, AC, Rogers, RL, Baumann, SB, Applications of magnetoenciphalography to the study of cognition, in (Ed.) Zappulla,

Figure 15. QEEG cognitive network map. *(From Gevins & Illes, 1991, reprinted with permission.)*

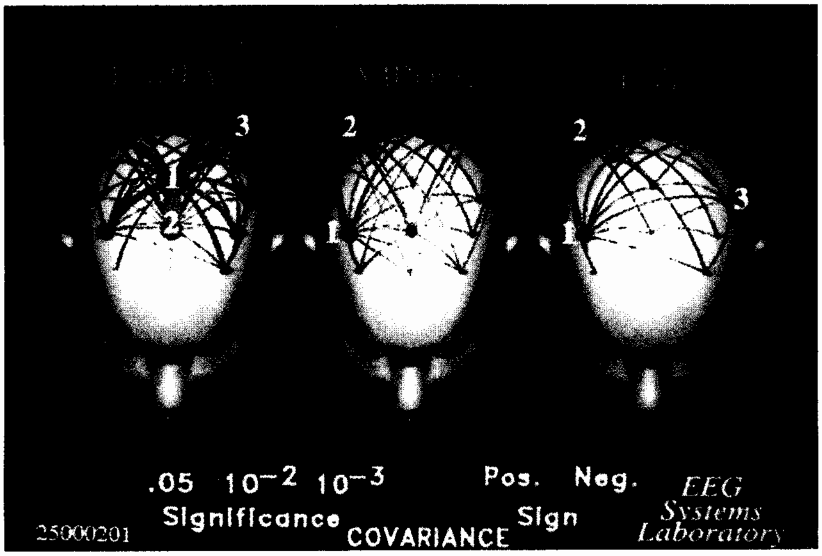

Pattern recognition analysis using an artificial, layered neural network that distinguished ERC neuroelectric patterns recorded during baseline (early), incipient performance impairment (middle), and impaired performance (late) periods from five Air Force test pilots performing a difficult visuomotor-memory task over a 14-h period. Baseline data were obtained during the first 7 hours; incipient performance impairment data during hours 7-10 preceding impaired performance; the impaired performance data were obtained during hours 10-14. The ERCs were measured during a 500-msec interval when the subjects were remembering two numbers and preparing for the next stimulus. ERCs greatly declined in magnitude from baseline (early) to incipient performance impairment (middle) to impaired performance (late) epochs. The patterns also changed, with the emphasis shifting from the (1) midline central, (2) midline precentral, and (3) left parietal sites to right hemisphere sites.

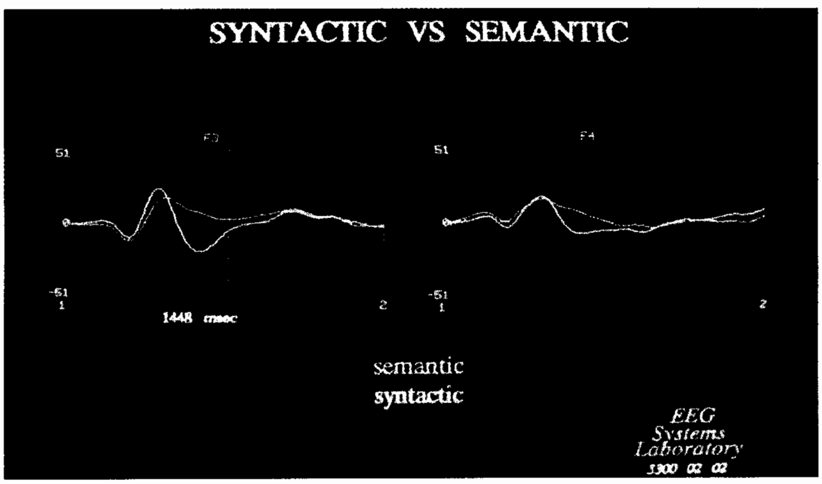

LD waveforms evoked by the first of two stimuli (syntactic and semantic) in an experiment designed to study elementary language processes. The waveforms are averaged across nine subjects. The major difference between the grammatic (syntactic) and semantic conditions is lateralized to the left hemisphere, where the grammatic condition has a substantial peak at 442 msec at left frontal and anterior central sites. The x-axis shows 1-sec beginning with the S1. The y-axis corresponds to ± 0.153 μ V/sq cm.

RA, LeFever, FF, Jaeger, J, Bilder, R, *Windows on the Brain*, 1991, *620*:118-127, New York:Annals of the New York Academy of Science.

Parks, RW, Lowwenstein, DA, Dodrill, KL, Barker, WW, Yoshii, F, Chang, JY, Cerebral metabolic effects of verbal fluency test: a PET scan study, *J Clin Exp Neuropsychol (Netherlands)*, 1988, *10*:565-575.

Pelizzari, CA, Chen, GTY, Halpern, H, Chen, C-T, and Cooper, MD, Three-dimensional correlation of PET, CT, and MRI images, *J Nucl Med*, 1987, *28* (suppl 1):528.

Petersen, SE, Fox, PT, Posner, MI, Mintun, M, Raichle, ME, Positron emission tomographic studies of the cortical anatomy of single-word processing, *Nature*, 1988, *331*:585-589.

Pieniadz, JM, Naeser, MA, Koff, E, Levine, HL, CT scan cerebral hemispheric asymmetry measurements in stroke cases with global aphasia: atypical asymmetries associated with improved recovery, *Cortex*, 1983, *19*:371-391.

Plante, E, MRI findings in the parents and Siblings of specifically language-impaired boys, *Brain and Lang*, 1991, *41*:67-80.

Plante, E, Swisher, L, Vance, R, Rapcsak, S, Anatomical correlates of normal and impaired language in a set of dizygotic twins, *Brain and Lang*, 1989, *37*:643-655.

Plante, E, Turkstra, L, Sources of error in the quantitative analysis of MRI scans, *Magnetic Res Imaging*, 1991, *9*:589-595.

Poole, KD, Devous, MD, Freeman, FJ, Watson, BC, Finitzo, T, Regional cerebral blood flow in developmental stutterers, *Arch Neurol*, 1991, *48*:509-512.

Purcell, EM, Torrey, HC, Pound, RV, Resonance absorption by nuclear magnetic moments in a solid, *Phys Rev*, 1946, *69*:37-38.

Raichle, M, Grubb, RL, Gado, MH, Eichling, JO, Ter-Pogossian, MM, Correlation between regional cerebral blood flow and oxidative metabolism, *Arch Neurol*, 1976, *33*:523-526.

Risberg, J, Ingvar, DH, Patterns of activation in the grey matter of the dominant hemisphere during memorizing and reasoning, *Brain*, 1973, *96*:737-756.

Figure 16. Magnetic field and electric potential field patterns produced by a current dipole. *(From Sams & Hari, 1991, p. 104, reprinted with permission.)*

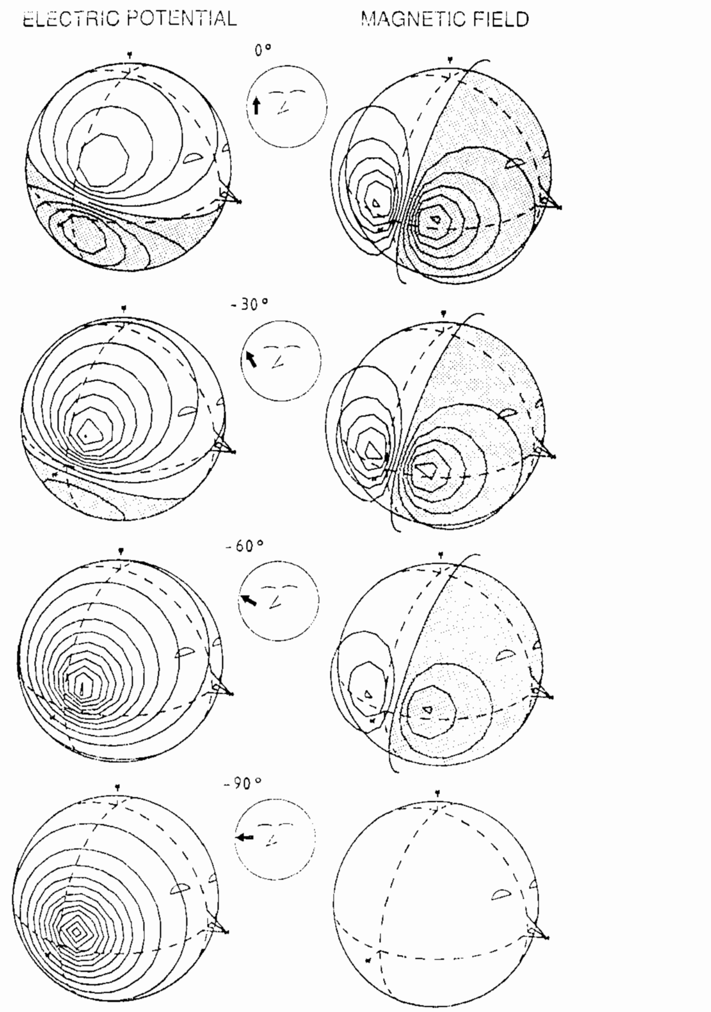

Magnetic field and electric potential field patterns produced by a current dipole (strength 20 nA·m) 20 mm below the surface of a sphere simulating the head. The dipole is assumed to be located in the supratemporal auditory cortex. The sphere contains four concentric layers with different electric conductivities. The outside radii (r) and conductivities (s) of the different layers are for brain: r = 92 mm, s = 0.33 1/Ωm; for cerebrospinal fluid: r = 94 mm, s = 1.40 1/Ωm; for skull: r = 102 mm, s = 0.006 1/Ωm; and for scalp: r = 106 mm, s = 0.28 1/Ωm. The current dipole is progressively tilted from the purely tangential (0°) to the purely radial (−90°) orientation, as indicated in the small schematic heads. The isocontour lines are separated by 0.5 μV for the electric potential and by 80 fT for the magnetic field patterns. The areas with positive electric potential and magnetic flux coming out of the head are shadowed.

Risberg, J, Ali, Z, Wilson, EM, Wills, Halsey, JH, Regional cerebral blood flow by ^{133}xenon inhalation, *Stroke*, 1975, *6*:142-148.

Risberg, J, Maximilian, AV, Prohovnik, I, Changes of cortical activity patterns during habituation to a reasoning test, *Neuropsychologica*, 1977, *15*:793-798.

Rodrigues, G, Cogorno, P, Gris, A, Marenco, S, Mesiti, C, Nobili, F, Rosadini, G, Regional cerebral blood flow and anxiety: a correlation study in neurologically normal patients, *J Cereb Blood Flow Metab*, 1989, *9*:410-416.

Roland, PE, Larsen, B, Focal increase of cerebral blood flow during stereognostic testing in man, *Arch Neuol*, 1976, *33*:551-558.

Roland, FE, Larsen, B, Skinhoj, E, Lassen, NA, Regional cerebral blood flow increase due to treatment of somatosensory and auditive information in mam, *Acta Neurological Scand*, 1977, *64*:540-541.

Romani, GL, Advances in neuromagnetic topography and source localization, *Brain Topogr*, 1990, *3*:95-102.

Romani, GL, Pizzella, V, Localization properties of multi-senson biomagnetic systems, *Acta Otolaryngol Suppl (Stockh)*, 1991, *491*:43-51.

Ropper, AH, A preliminary MRI study of the geometry of brain displacement and level of consciousness with acute intracranial masses, *Neurology*, 1989, *39*:622-627.

Sams, M, Hari, R, Magnetoencephalography in the study of human auditory information processing, in (Ed.) Zappulla, RA, LeFever, FF, Jaeger, J, Bilder, R, *Windows on the Brain*, 1991, *620*:102-117, New York:Annals of the New York Academy of Science.

Shedlack, KJ, Hunter, R, Wyper, D, McLuskie, R, Fink, G, Goodwin, GM, The pattern of cerebral activity underlying verbal fluency shown by split-dose single photon emission tomography (SPET or SPECT) in normal volunteers, *Psychol Med*, 1991, *21*:687-696.

Starr, A, Kristeva, R, Cheyne, D, Lindinger, G, Deecke, L, Localization of brain activity during auditory verbal short-term memory derived from magnetic recordings, *Brain Res*, 1991, *558*:181-190.

Steinmetz, H, Seitz, RJ, Functional anatomy of language processing: neuroimaging and the problem of individual variability, *Neuropsychologica*, 1992, *29*:114-1161.

Thaller, RA, Petsche, H, Rappelsberger, P, Pockberger, H, Lindner, K, Imhof, H, An approach to a synopsis of EEG parameters, morphology of brain convolutions and mental activities, *Brain Topogr*, 1991, *4*:65-73.

Thatcher, RW, Walker, RA, Guidice, S, Human cerebral hemispheres develop at different rates and ages, *Science*, 1987, *236*:1110-1113.

Terayama, Y, Meyer, JS, Kawamura, J, Weathers, S, Role of thalamus and white matter in cognitive outcome after head injury, *J Cereb Blood Flow Metab*, 1991, *11*:852-860.

Figure 17. The measurement of neuromagnetic signals of the human brain with SQUID sensors. *(From Hari & Lounasmaa, 1989, reprinted with permission.)*

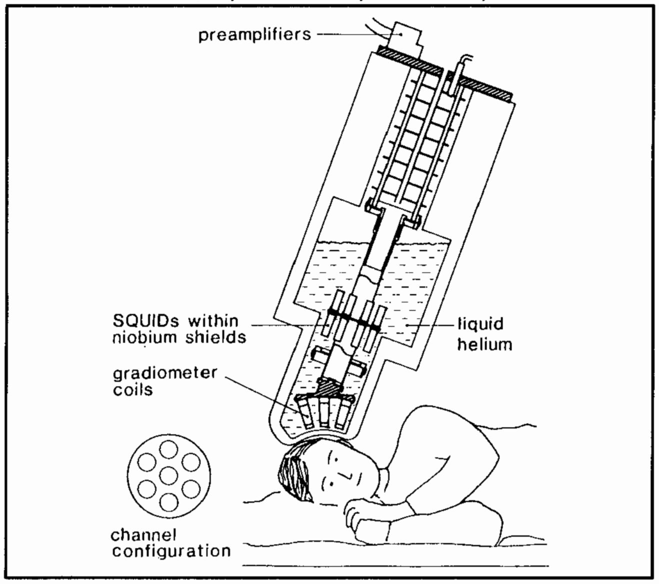

Figure 18. Seven simultaneoulsy measured averaged responses (N=500) from the locations indicated in the schematic head. The top portion shows a dipolar current source located in the auditory cortex and the magnetic field generated by it. The P50m and N100m responses are of opposite polarities at channels 2 and 5, suggesting a dipolar source between these sites in the underlying cortex. The stimui were 1000 Hz sinusoids (90 dB, 100 ms) repeated once every 510 ms. *(From Sams & Hari, 1991, reprinted with permission.)*

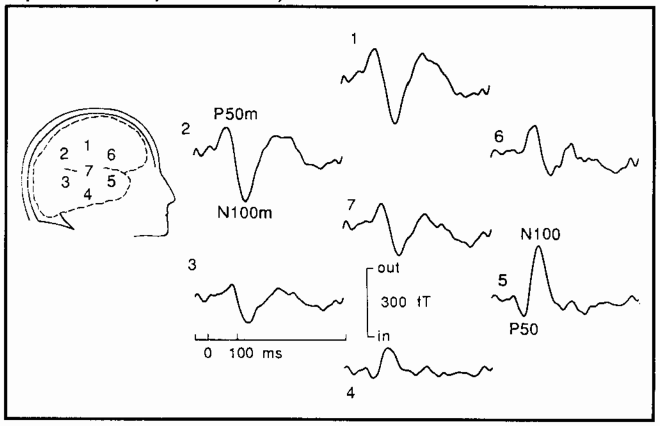

Walshe, TM, Davis, KR, Fisher, CM, Thalamic hemorrahage: a computer tomographic-clinical correlation, *Neurology*, 1977, *27*:217-222.

Wang, PP, Doherty, S, Hesselink, JR, Bellugi, U, Callosal morphology concurs with neruobehavioral and neuropathological findings in two neurodevelopmental disorders, *Arch Neurol*, 1992, *49*:407-411.

Watson, RT, Fleet, S, Gonzalez-Rothi, L, Heilman, KM, Apraxia and the supplementary motor area, *Arch Neurol*, 1986, *43*:787-792.

Williamson, SJ, Lu, ZL, Karron, D, Kaufamn, L, Advantages and limitations of magnetic source imaging, *Brain Topogr*, 1991, *4*:169-180.0

Wood, F, Taylor, B, Penny, R, Stump, D, Regional cerebral blood flow response to recognition memory versus semantic classification tasks, *Brain and Lang*, 1980, *9*:113-122.

Wood, F, McHenry, L, Roman-Campos, G, Poser, CM, Regional cerebral blood flow response in a patient with remitted global amnesia, *Brain and Lang*, 1980, *9*:123-128.

Wrenn, FR, Good, ML, Handler, P, The use of positron emitting radioisotopes in nuclear medicine imaging, *Science*, 1951, *113*:525-527.

Vallar, G, Perani, D, The anatomy of unilateral neglect after right-hemisphere stroke lesions: a clinical/CT scan correlation study in man, *Neuropsychologica*, 1986, *24*:609-622.

Volkow, ND, Mullani, NA, and Bendriem, B, Positron Emission Tomography Instrumentation: An Overview, *Am J Physiol Imaging*, 1988, *3*:142-153.

Webb, S, *The Physics of Medical Imaging*, 1988, Bristol:Adam Hilger, Ltd.

Zappulla, RA, LeFever, FF, Jaeger, J, Bilder, R, (Eds), *Windows on the Brain*, 1991, *620*, New York:Annals of the New York Academy of Science.

Zappulla, RA, Fundamentals and applications of quantified electrophysiology, in (Ed.) Zappulla, RA, LeFever, FF, Jaeger, J, Bilder, R, *Windows on the Brain*, 1991, *620*:1-21, New York:Annals of the New York Academy of Science.

Figure 19. Region of Interest map. *(From Evans, et al., 1988, reprinted with permission.)*

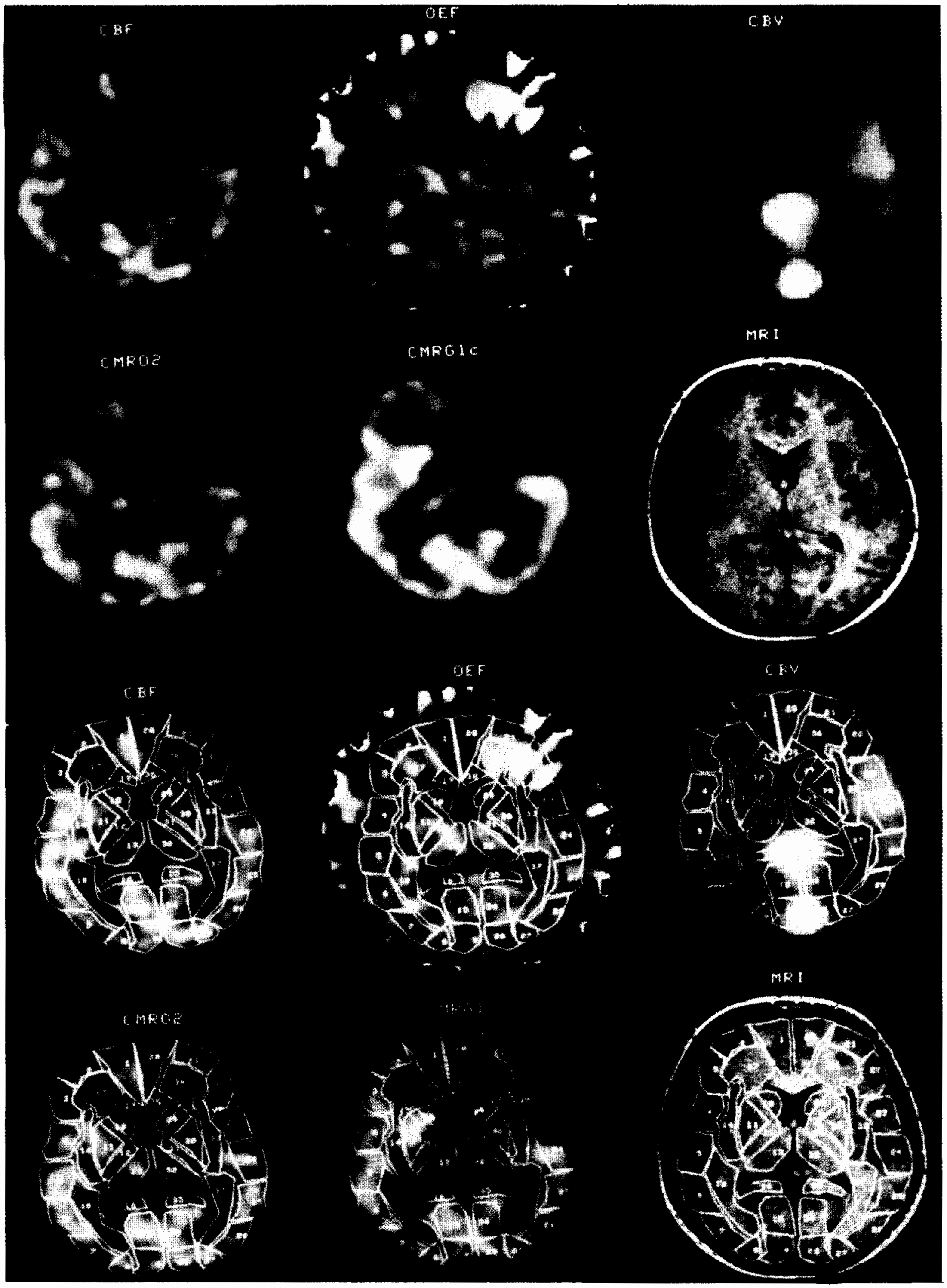

Sample region of interest template for a multifunctional study in stroke. In this case of ischemic infarction, the top set of images show the typical appearance of PET images for CBF, OEF, CBV, $CMRO_2$, and CMRGlc in such cases plus the corresponding MRI anatomical image. The lower set shows the same data with a region of interest template derived from the atlas and customized to this slice. A free region was also defined to indicate the infarction site using a combination of the MRI and PET data to define the physical and functional limits of the infarct. The presence of the template on the CBV image clearly shows the extent of volume averaging for structures near the sagittal sinus and the internal cerebral vein. CBV values from such structures can be automatically excluded from subsequent analysis.